VIA MEDICA

ORIGINAL ARTICLE

Folia Morphol.
Vol. 83, No. 3, pp. 656–666
DOI: 10.5603/fm.96874
Copyright © 2024 Via Medica
ISSN 0015–5659
eISSN 1644–3284
journals.viamedica.pl

Adipocyte enhancer binding protein 1 exacerbates myocardial ischaemia-reperfusion injury via inhibition of IκBα

Wei-Na Xue

Cath Lab, Zhangjiakou First Hospital, Zhangjiakou, Hebei Province, P.R. China

[Received: 8 August 2023; Accepted: 11 September 2023; Early publication date: 31 October 2023]

Myocardial ischaemia/reperfusion injury (MIRI) remains a major cause of death after cardiovascular diseases. Up-regulation of adipocyte enhancer binding protein 1 (AEBP1) has been found in ischaemic cardiomyopathy patients. However, its influence and detailed mechanisms in MIRI are obscure. In this study, expression of target molecules was determined by RT-qPCR and Western blotting. Cell viability and apoptosis were evaluated by CCK-8 and TUNEL. Inflammatory cytokine levels were assessed by ELISA. Myocardial function and pathological changes were examined by echocardiography and HE staining. Cardiac infarct size was determined by TTC staining. Our data indicate that oxygen-glucose deprivation/reoxygenation (OGD/R) resulted in high expression of AEBP1 but low expression of IκBα in cardiomyocytes. In vitro data indicate that AEBP1 knockdown increased viability, and inhibited apoptosis and inflammation in H9c2 cells under OGD/R. AEBP1 interacted with IκBα to cause IκBα degradation and facilitated the nuclear translocation of NF-κB. Moreover, IκBα silencing attenuated siAEBP1-medaited inhibition in inflammation and apoptosis of OGD/R-treated H9c2 cells, suggesting that IκBα was involved in the pro-inflammatory action of AEBP1. Finally, deficiency of AEBP1 mitigated MIRI in rats through IκBα/NF-κB pathway. Taken together, AEBP1 exacerbated MIRI through repressing IκBα expression to trigger NF-κB-mediated inflammation. (Folia Morphol 2024; 83, 3: 656–666)

Keywords: myocardial ischaemia-reperfusion injury, AEBP1, IκBα, NF-κB, inflammation, apoptosis

INTRODUCTION

Myocardial ischaemia/reperfusion injury (MIRI) after restoration of blood flow to the ischaemic heart can cause irreversible myocardial damage [7]. MIRI remains a severe threat to human beings, and the mortality rate of patients with MIRI is as high as 7% [29]. The occurrence and development of MIRI is a complex process modulated by complicated mechanisms [19]. Therefore, it is of great significance to explore the mediators and molecular mechanisms underlying MIRI.

Adipocyte enhancer binding protein 1 (AEBP1) was originally identified as a transcriptional repressor of the adipose P2 gene in adipocytes [15]. High expression of AEBP1 in macrophages has been reported to trigger the release of various pro-inflammatory cytokines, such as interleukin 6 (IL-6) and tumour necrosis factor alpha (TNF-α) [10]. Furthermore, functioned

Address for correspondence: Wei-Na Xue, Cath Lab, Zhangjiakou First Hospital, No. 6, Qiaoxi District, Zhangjiakou 075000, Hebei Province, P.R. China; tel: +86-18031355099, e-mail: xwn691382821@163.com

This article is available in open access under Creative Common Attribution-Non-Commercial-No Derivatives 4.0 International (CC BY-NC-ND 4.0) license, allowing to download articles and share them with others as long as they credit the authors and the publisher, but without permission to change them in any way or use them commercially.

as a transcriptional suppressor, AEBP1 is implicated in the modulation of multiple pathophysiological processes, such as tumourigenesis and inflammation [8, 14]. A recent study found that AEBP1 was up-regulated in ischaemic cardiomyopathy patients [16]. Also, AEBP1 was demonstrated as a key promoter of cardiac fibrosis in heart failure [13]. However, the biological function of AEBP1 in MIRI and its detailed mechanisms remain obscure, which deserves to be investigated.

Nuclear factor kappa B (NF-κB) is a transcription factor that induces inflammatory response in a variety of cells. Accumulated studies have suggested that activation of NF-κB resulted in severe inflammatory injury in myocardial tissue during MIRI [25, 28]. Inactivation of NF-κB can effectively repress inflammation, thereby providing cardiac protection [27]. Inhibitor of κB alpha (IκBα) can bind to cytoplastic NF-κB p65/ /p50 heterodimer under normal conditions, which is considered as an inhibitor of NF-κB. Upon stimulation, IκBα is degraded via proteasomal pathway and consequently leads to NF-κB p65 nuclear translocation and activation [27]. Interestingly, previous studies have reported that AEBP1 could interact with IκBα to repress IκBα expression [2, 11]. Therefore, we predicted that AEBP1 might exacerbate MIRI via target repression of IκBα expression to trigger NF-κB--induced inflammation.

In this study, we aimed to investigate the role of AEBP1/IκBα axis in MIRI development in the *in vitro* and *in vivo* experimental models. Our findings provide new insights into the function of AEBP1 in MIRI.

MATERIALS AND METHODS

Cell culture and treatment

H9c2 cells were provided by American Type Culture Collection (ATCC, Manassas, VA, USA) and maintained in Dulbecco's modified Eagle medium (DMEM) containing 10% foetal bovine serum at 37°C with 5% CO_2. Oxygen-glucose deprivation/reoxygenation (OGD/R) was performed on H9c2 cells to simulate MIRI *in vitro* as described before [3]. In brief, H9c2 cells were cultured in DMEM without serum and glucose under hypoxia conditions (95% N_2, 5% CO_2) for 2, 4, 8, and 12 h. Subsequently, H9c2 cells were maintained in DMEM complete medium under normoxic condition for 24 h.

Cell transfection

siRNA targeting AEBP1 (siAEBP1), siIκBα, negative control siRNA (siNC), overexpression plasmid for AEBP1 (OE-AEBP1), and OE-vector were purchased from GeneChem (Shanghai, China). These segments were transfected into H9c2 cells using Lipofectamine 2000 (Thermo Fisher, Waltham, MA, USA).

Cell counting kit-8 (CCK-8)

H9c2 cells were planted into 96-well plates (1×10^4 cells per well). After various treatments, H9c2 cell viability was measured using the Enhanced Cell Counting Kit 8 (Elabscience, Wuhan, China), as previously described [23]. Briefly, the cells were added with 10 μL of CCK-8 solution, followed by incubation at 37°C for 3 h. The results were obtained at 450 nm using a microplate reader (Molecular Devices, San Jose, CA, USA).

TUNEL

Apoptosis was evaluated using the One-step TUNEL In Situ Apoptosis Kit (Green, Elab Fluor 488) and One-step TUNEL In Situ Apoptosis Kit (Red, Elab Fluor 594) (Elabscience). For myocardial tissues, the paraffin sections were subjected to dewaxing, rehydration, proteinase K, and 3% hydrogen peroxide treatment. The sections were reacted with the TUNEL reaction mixture. For H9c2 cells, the cell monolayers were mounted on coverslips, followed by proteinase K treatment and incubation with the TUNEL reaction mixture. After nuclear staining with DAPI, the labelled apoptotic cells were observed with a fluorescence microscope (Olympus, Tokyo, Japan).

Enzyme-linked immunosorbent assay (ELISA)

The levels of LDH, CK-MB, TNF-α, IL-1β, and IL-6 in the cellular supernatant or serum samples were evaluated using the commercial ELISA kits for lactate dehydrogenase (LDH, SEB864Ra), creatine kinase MB isoenzyme (CK-MB, SEA479Ra), tumour necrosis factor alpha (TNFa, SEA133Ra), interleukin 1 beta (IL1b, SEA563Ra), and interleukin 6 (IL6, SEA079Ra), following the instructions.

Quantitative reverse transcription PCR (RT-qPCR)

RT-qPCR was performed as described before [26]. In brief, total RNA was extracted from H9c2 cells using the TRIzol reagent (Thermo Fisher), and subsequently transcribed into cDNA using the Transcriptor First Strand cDNA Synthesis Kit (Thermo Fisher). qPCR was conducted using the SYBR Green PCR Kit (QIAGEN, Germany), with GAPDH used as an internal reference control. The PCR primer sequences are shown in

Table 1. Oligonucleotide primer sets for RT-qPCR.

Name	Sequence (5'¬3')	Length
AEBP1 F	CATCCGCATCTATCCACTAC	20
AEBP1 R	ACCTCATCCTCGTCTTCTCC	20
IκBα F	CGTGTCTGCACCTAGCCTCTATC	23
IκBα R	GCGAAACCAGGTCAGGATTC	20
GAPDH F	GACATGCCGCCTGGAGAAAC	20
GAPDH R	AGCCCAGGATGCCCTTTAGT	20

Table 1. The relative expression of genes was analysed using the $2^{-\Delta\Delta Ct}$ method.

Western blotting

Western blotting was conducted according to a previous study [21]. Briefly, cells were lysed in the RIPA Lysis Buffer (Absin, Shanghai, China). Total protein in the supernatant was collected after centrifugation and quantified using the BCA assay kit (Absin). Then, the protein samples were subjected to SDS-PAGE and blotted onto polyvinylidene fluoride membranes. After blocking in defatted milk, the membranes were incubated with primary antibodies, including AEBP1 (A16340, 1:1000, ABclonal, Wuhan, China), IκBα (A11397, 1:500, ABclonal), NF-κB p65 (A2547, 1:500, ABclonal), β-actin (AC006, 1:500, ABclonal), and histone H3 (A2348, 1:2000, ABclonal) at 4°C overnight, followed by probing with secondary antibody for 1 h. The protein blots were detected using the ECL kit (Absin).

Co-immunoprecipitation (Co-IP)

Co-IP was performed as described previously [12]. Briefly, whole cell lysates were prepared using the RIPA Lysis Buffer, followed by centrifugation at 10,000 g for 10 min at 4°C. Thereafter, the cell lysates were immuno-precipitated with anti-IκBα (A11397, 1:20, ABclonal), or anti-IgG antibody (1:100, Cell Signalling Technology, Danvers, MA, USA) for 16 h, and then incubated with protein A/G agarose beads (Thermo Fisher) overnight at 4°C. Then, the immunocomplexes were spun down, recovered, and boiled for 10 min at 100°C. The protein levels of AEBP1 and IκBα were assessed by Western blotting.

Animal model

All animal experiments were carried out in accordance with the NIH guidelines and approved by the Institutional Animal Care and Use Committee of Zhangjiakou First Hospital. Male Sprague Dawley rats (200–250 g) were provided by Charles River Laboratories (Beijing, China) and randomly assigned to Sham, MIRI, MIRI + siNC, MIRI + siAEBP1, or MIRI + + siAEBP1 + siIκBα groups (n = 6 per group). MIRI was induced by left anterior descending artery (LAD) ligation. Briefly, the rats were anaesthetised with pentobarbital (30 mg/kg, intraperitoneally) and then received left thoracotomy. The LAD was ligated using a 6–0 silk suture for 30 min. Subsequently, the ligature wire was loosened to achieve myocardial reperfusion. Sham rats received the same surgery without LAD ligation. For *in vivo* transfection, siAEBP1, siIκBα, or siNC (50 μg) dissolved in the *in vivo*-jetPEI reagent (Polyplus-transfection, USA) were injected into the left ventricle anterior wall of rats 48 h before MIRI induction [17]. All rats were euthanised by an overdose of pentobarbital (120 mg/kg, intravenously). The serum and heart samples were collected for further analysis.

Cardiac function

Cardiac function of rats was evaluated by echocardiography using Vevo 2100 (VisualSonics, Toronto, Canada). Left ventricular ejection fraction (LVEF) and left ventricular fraction shortening (LVFS) were detected from at least 3 consecutive cardiac cycles.

2,3,5-triphenyltetrazolium chloride (TTC) staining

After washing by saline, 0.3% Evans Blue staining solution was injected into the aorta. The hearts were cut into 1.5-mm sections, followed by staining with 1% TTC at 37°C for 20 min. The infarct area was analysed using a light microscope (Olympus) and quantified by Image-Pro Plus 5.0 software.

Haematoxylin and eosin (H&E) staining

The heart tissues were fixed with 10% formaldehyde solution, embedded in paraffin, and sliced into 5 μm sections. The prepared sections were stained using the H&E staining kit (Sangon, Shanghai, China). Images were photographed under a light microscope.

Statistical analysis

Data are presented as mean ± standard deviation (SD). GraphPad Prism 6.0 was adopted for statistical analysis using Student's t test for 2-group or One-Way ANOVA for multiple-group comparison. A p-value less than 0.05 was considered as statistically significant.

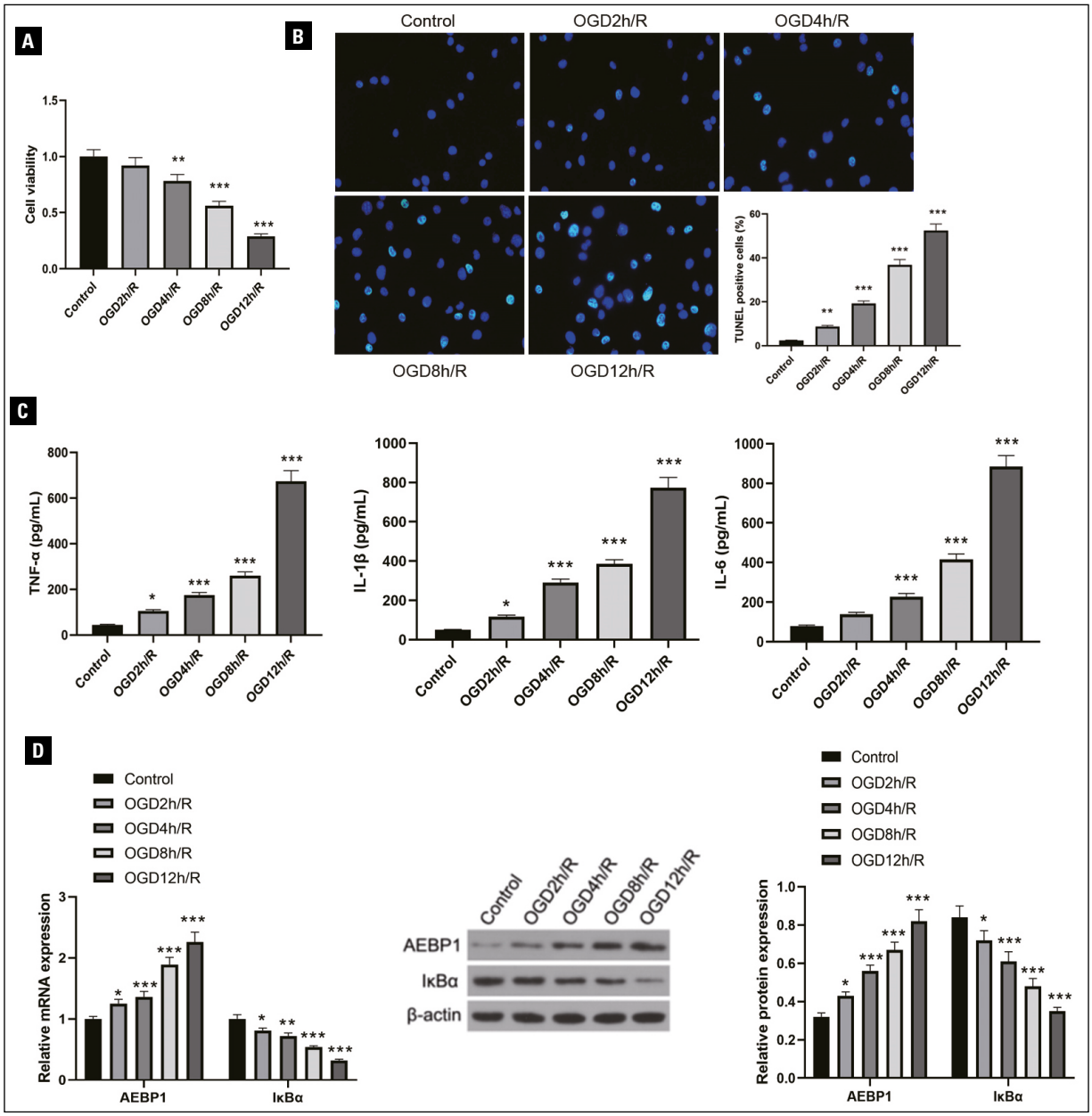

Figure 1. AEBP1 was up-regulated, but IκBα was down-regulated in OGD/R-exposed cardiomyocytes. H9c2 cells were subjected to OGD for 2, 4, 8, and 12 h, followed by reperfusion for 24 h. **A.** H9c2 cell viability was assessed by CCK-8. **B.** Apoptotic percentage of H9c2 cells was evaluated by TUNEL. **C.** Release of TNF-α, IL-1β, and IL-6 from H9c2 cells was determined by ELISA. **D.** AEBP1 expression was measured by RT-qPCR and Western blotting. Data are expressed as mean ± SD. *$p < 0.05$, **$p < 0.01$, ***$p < 0.001$. AEBP1 — adipocyte enhancer binding protein 1; CCK-8 — cell counting kit-8; IκBα — inhibitor of κB alpha; OGD/R — oxygen-glucose deprivation/reoxygenation; TNF-α — tumour necrosis factor alpha.

RESULTS

Up-regulation of AEBP1 and down-regulation of IκBα in OGD/R-exposed cardiomyocytes

First, H9c2 cardiomyocytes were stimulated with OGD/R to simulate HIRI *in vitro*. H9c2 cell viability was strikingly declined with prolonged OGD time (Fig. 1A). Meanwhile, the apoptotic percentage of H9c2 cells elevated from OGD 2 h to 12 h after reperfusion (Fig. 1B). Moreover, the release of TNF-α, IL-1β, and IL-6 from H9c2 cells was time dependently enhanced after OGD/R stimulation (Fig. 1C). Notably, the mRNA and protein levels of AEBP1 were enhanced, while IκBα levels were reduced in OGD/R-exposed H9c2 cells in a time-dependent manner (Fig. 1D). Thus, AEBP1 expression was increased, but IκBα expression was decreased during OGD/R-induced cardiomyocyte injury.

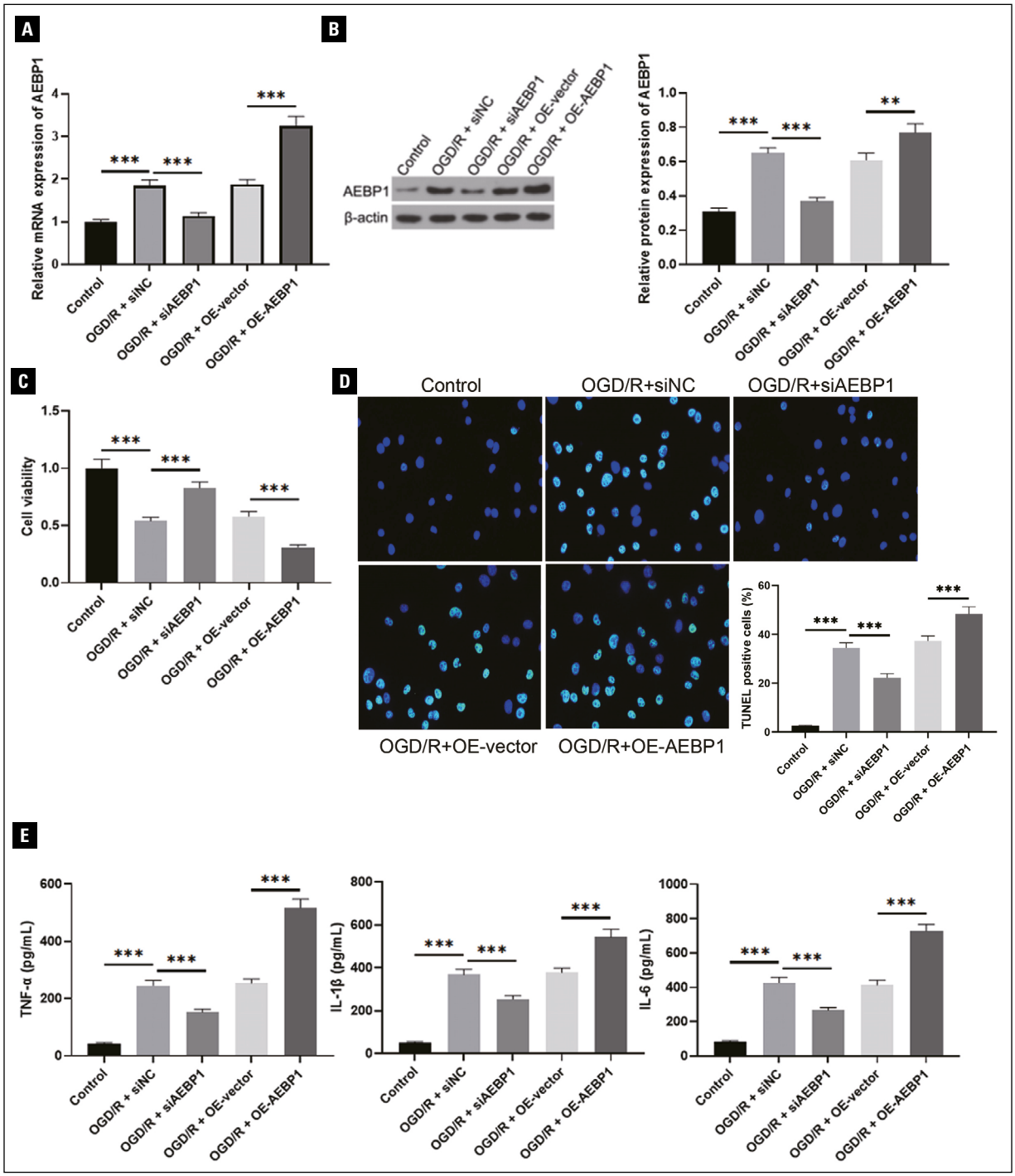

Figure 2. AEBP1 affected cardiomyocyte inflammation and apoptosis upon OGD/R stimulation. H9c2 cells were transfected with siAEBP1 or OE-AEBP1 and then stimulated by OGD/R. **A, B.** RT-qPCR and Western blotting analysis of AEBP1 expression in H9c2 cells. **C.** The viability of H9c2 cells from various groups was determined by CCK-8. **D.** Apoptosis of H9c2 cells was detected by TUNEL. **E.** The production of TNF-α, IL-1β, and IL-6 was assessed by ELISA. Data are expressed as mean ± SD. **p < 0.01, ***p < 0.001. AEBP1 — adipocyte enhancer binding protein 1; CCK-8 — cell counting kit-8; OGD/R — oxygen-glucose deprivation/reoxygenation; SD — standard deviation; TNF-α — tumour necrosis factor alpha.

AEBP1 modulated OGD/R-induced inflammation and apoptosis in cardiomyocytes

Given that AEBP1 was dysregulated by OGD/R stimulation, we further evaluated its influence on OGD/R-induced cardiomyocyte damage. For this purpose, H9c2 cells were transfected with siAEBP1 or OE-AEBP1, and then subjected to OGD/R. We found that the enhanced expression of AEBP1 in OGD/R-stimulated H9c2 cells was abolished by siAEBP1 transfection but intensified by OE-AEBP1 transfection (Fig. 2A, B). Functionally,

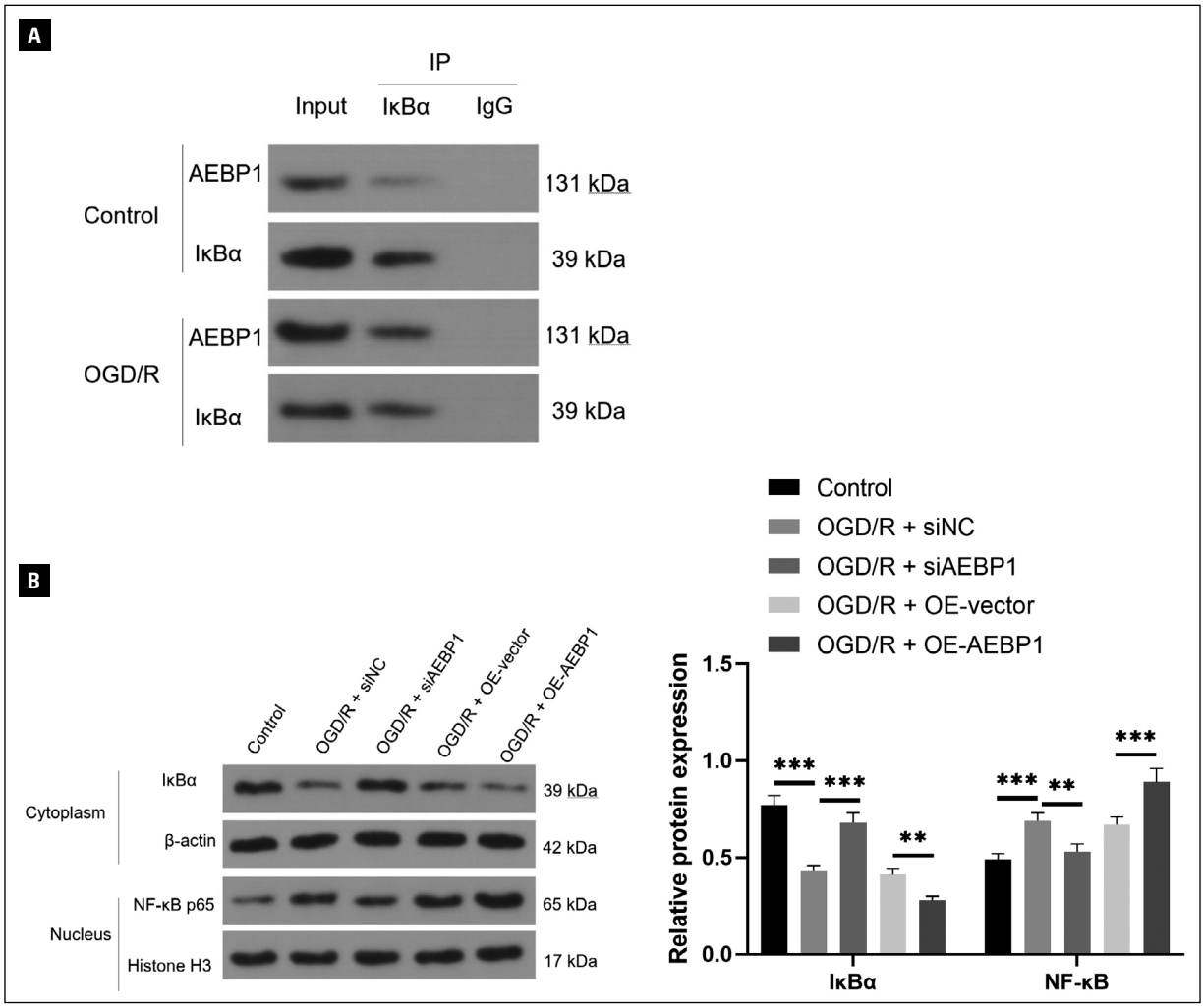

Figure 3. AEBP1 hampered IκBα expression to activate NF-κB pathway. **A.** The interaction between AEBP1 and IκBα proteins in H9c2 cells with or without OGD/R exposure was validated by Co-IP assay. **B.** The protein levels of IκBα and nuclear NF-κB p65 were evaluated by Western blotting. Data are expressed as mean ± SD. $^{**}p < 0.01$, $^{***}p < 0.001$. AEBP1 — adipocyte enhancer binding protein 1; IκBα — inhibitor of κB alpha; OGD/R — oxygen-glucose deprivation/reoxygenation.

knockdown of AEBP1 restored the decreased viability of OGD/R-challenged H9c2 cells, whereas AEBP1 overexpression led to the opposite result (Fig. 2C). In addition, apoptosis of H9c2 cells was restrained by AEBP1 silencing but promoted by AEBP1 overexpression in response to OGD/R (Fig. 2D). Furthermore, OGD/R-induced TNF-α, IL-1β, and IL-6 production was attenuated by AEBP1 deficiency but strengthened by AEBP1 overexpression (Fig. 2E). These observations suggested that high expression of AEBP1 contributed to OGD/R-induced inflammation and apoptosis in H9c2 cells.

AEBP1 repressed IκBα expression to trigger NF-κB activation

To further investigate the downstream regulatory mechanism of AEBP1 in OGD/R-induced cardiomyocyte injury, IκBα was focused on. Co-IP assay demonstrated that AEBP1 directly interacted with IκBα protein, which was enhanced by OGD/R challenge (Fig. 3A). Additionally, the elevated expression of nuclear NF-κB p65 and declined expression of IκBα were reversed in AEBP1-depleted H9c2 cells upon OGD/R stimulation. Conversely, AEBP1 overexpression further up-regulated nuclear NF-κB p65 but down-regulated IκBα (Fig. 3B). Therefore, AEBP1 directly interplayed with IκBα to inhibit its expression, thereby activating NF-κB pathway.

AEBP1 knockdown restrained OGD/R-induced inflammation and apoptosis via IκBα inhibition

Next, we verified whether the AEBP1/IκBα axis modulated OGD/R-induced inflammation and apop-

tosis in H9c2 cells. To achieve this, H9c2 cells were transfected with siAEBP1 with or without siIκBα. As shown in Fig. 4A, siAEBP1-mediated up-regulation of IκBα in OGD/R-exposed H9c2 cells was counteracted by IκBα knockdown. Moreover, inhibition of AEBP1-induced elevation in OGD/R-treated H9c2 cell viability was abrogated by IκBα silencing (Fig. 4B). Also, the anti-apoptotic role of siAEBP1 in H9c2 cells upon OGD/R stimulation was abolished by IκBα depletion (Fig. 4C). Additionally, co-transfection with siIκBα reversed AEBP1 deficiency-induced down-regulation of TNF-α, IL-1β, and IL-6 levels in the supernatant of OGD/R-challenged H9c2 cells (Fig. 4D). Taken together, AEBP1 depletion attenuated OGD/R-induced inflammation and apoptosis via down-regulation of IκBα.

AEBP1 down-regulation ameliorated MIRI in rats via the IκBα/NF-κB pathway

Finally, we validated the role of the AEBP1/IκBα axis in MIRI rats *in vivo*. The infarct volume of hearts from MIRI rats was remarkably increased, which could be reduced by AEBP1 knockdown. However, IκBα silencing counteracted the siAEBP1-induced decrease in infarct volume (Fig. 5A). HE staining indicated that MIRI triggered pathological alterations in the heart tissues, including inflammatory infiltration, necrosis, and structural abnormality. AEBP1 depletion attenuated these pathological damages, which was abolished by IκBα deficiency (Fig. 5B). In addition, the elevated levels of myocardial enzymes LDH and CK-MB indicated myocardial injury of MIRI rats. AEBP1 down-regulation effectively reduced serum LDH and CK-MB levels of MIRI rats, whereas co-inhibition of IκBα significantly raised LDH and CK-MB levels (Fig. 5C, D). In addition, cardiac function was improved in AEBP1-silenced rats via enhancement of LVEF and LVFS levels, which was counteracted after IκBα depletion (Fig. 5E). Moreover, the apoptosis in myocardial tissues of MIRI rats was weakened by AEBP1 deficiency, whereas IκBα silencing reversed the anti-apoptotic effect of siAEBP1 (Fig. 5F). Also, the enhanced serum TNF-α, IL-1β, and IL-6 levels of MIRI rats were down-regulated by AEBP1 knockdown; however, these pro-inflammatory cytokine levels were elevated by co-silencing of IκBα (Fig. 5G). Western blotting revealed that up-regulation of AEBP1 and nuclear NF-κB p65, and down-regulation of IκBα in heart tissues of MIRI rats were reversed in AEBP1-depleted rats, which were abrogated when IκBα was knocked down (Fig. 5H). The above results suggest that AEBP1 depletion attenuated MIRI in rats via promotion of IκBα-mediated inactivation of NF-κB.

DISCUSSION

MIRI has been recognised as a dangerous pathological process after reperfusion therapy in myocardial infarction patients [24]. Identification of the mechanisms and protective measures of MIRI has become a hotspot in this field of medicine. In this study, we found that AEBP1 was highly expressed during OGD/R-induced cardiomyocyte inflammation and apoptosis. Subsequently, we verified that AEBP1 silencing blocked OGD/R-induced cardiomyocyte injury, while AEBP1 overexpression exacerbated OGD/R-triggered cardiomyocyte damage. In addition, AEBP1 knockdown promoted IκBα expression to inactivate NF-κB pathway in OGD/R-stimulated H9c2 cells, and depletion of IκBα reversed AEBP1 deficiency-induced cardioprotective effects *in vitro* and *in vivo*. Therefore, our findings demonstrated that AEBP1 inhibition ameliorated MIRI via increased IκBα expression.

MIRI can be caused by inflammation via complicated molecular mechanisms [22]. It has been proven that inflammation is a distinct feature of MIRI, which drives cardiomyocyte apoptosis and injury [1, 18]. Mounting evidence has identified that a great deal of immune cells are infiltrated in myocardial tissue during MIRI, and they produce large amounts of pro-inflammatory cytokines, including TNF-α, IL-1β, and IL-6 [18]. Myocardial inflammation after MIRI exerts a crucial role in aggravating cardiac dysfunction and results in a bad prognosis of myocardial infarction patients. Thus, anti-inflammatory therapy represents a key strategy to attenuate MIRI [20]. AEBP1 is a transcriptional regulator that is implicated in the modulation of various biological processes including inflammation [9]. For example, AEBP1 facilitated macrophage inflammatory responsiveness via increasing NF-κB activity during mammary epithelial cell hyperplasia [6]. Ren et al. documented that AEBP1 acted as a driver of inflammation, which contributed to the pathological development of abdominal aortic aneurysm [14]. In line with these studies, we discovered that down-regulation of AEBP1 restrained myocardial inflammation and apoptosis in MIRI models. Overall, our results demonstrated, for the first time, AEBP1 as a potential treatment target for MIRI.

Next, we focused on the detailed molecular mechanism through which AEBP1 enhanced myocardial inflammatory response in MIRI. A previous study

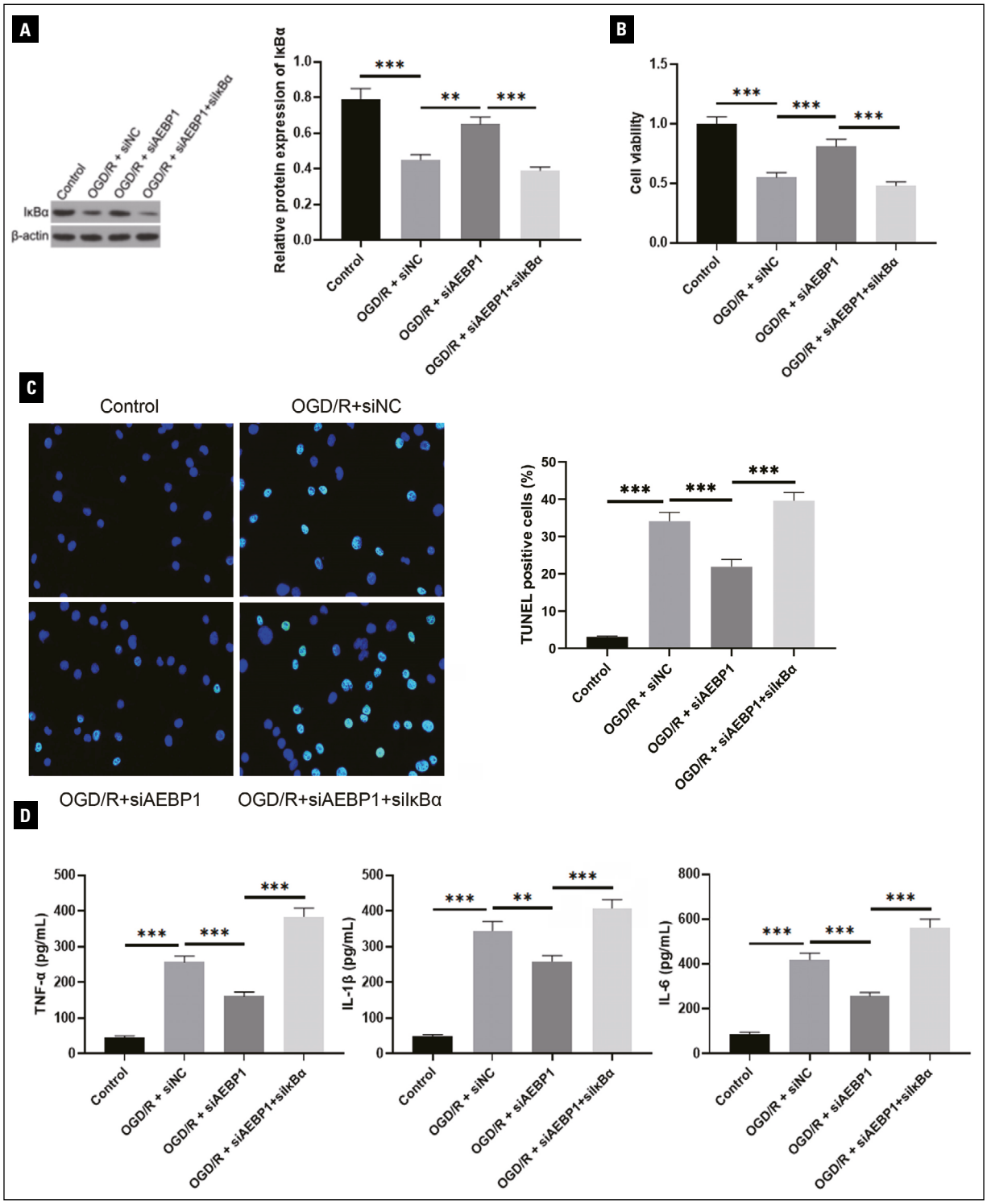

Figure 4. AEBP1 silencing relieved OGD/R-induced inflammation and apoptosis via inhibiting IκBα expression. OGD/R-challenged H9c2 cells were transfected with siAEBP1 combined with or without silκBα. **A.** Protein level of IκBα was assessed by Western blotting. **B.** CCK-8 assay evaluated H9c2 cell viability. **C.** The percentage of apoptotic H9c2 cells was measured by TUNEL. **D.** TNF-α, IL-1β, and IL-6 levels in the supernatant of H9c2 cells were determined by ELISA. Data are expressed as mean ± SD. $^{**}p < 0.01$, $^{***}p < 0.001$. AEBP1 — adipocyte enhancer binding protein 1; CCK-8 — cell counting kit-8; IL — interleukin; OGD/R — oxygen-glucose deprivation/reoxygenation; SD — standard deviation; TNF-α — tumour necrosis factor alpha.

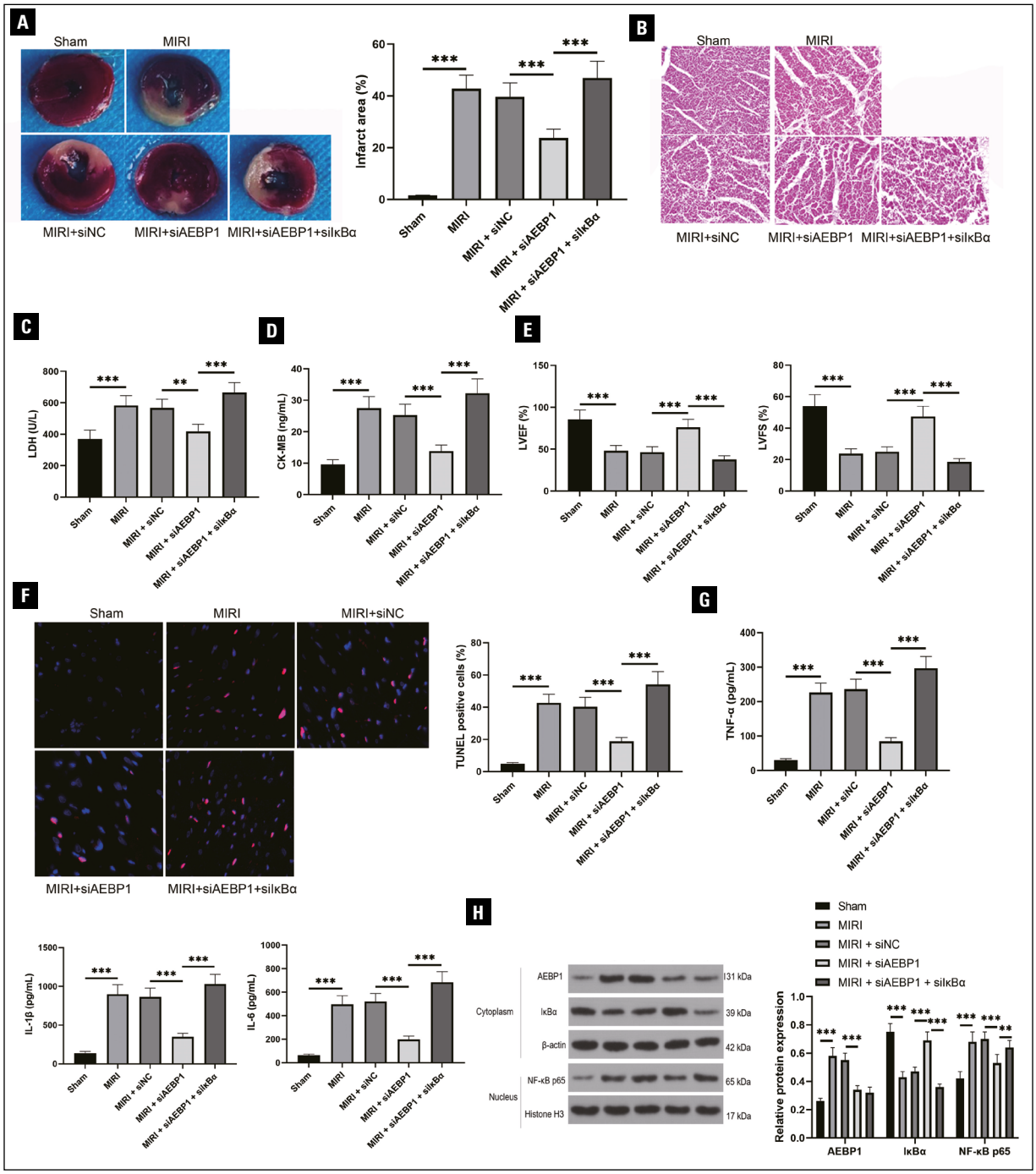

Figure 5. AEBP1 deficiency attenuated MIRI in rats via regulation of IκBα/NF-κB pathway. **A.** The infarct area of heats was measured by TTC staining. **B.** H&E staining evaluated the pathological alterations in heart tissues. **C, D.** The serum levels of LDH and CK-MB were detected by ELISA. **E.** LVEF and LVFS were assessed by echocardiography to determine cardiac function. **F.** TUNEL was performed to detect apoptosis in myocardial tissues. **G.** The serum levels of TNF-α, IL-1β, and IL-6 were detected by ELISA. **H.** The protein abundance of AEBP1, IκBα, and nuclear NF-κB p65 was evaluated by Western blotting. Data are expressed as mean ± SD. $^{**}p < 0.01$, $^{***}p < 0.001$. AEBP1 — adipocyte enhancer binding protein 1; CCK-8 — cell counting kit-8; H&E — haematoxylin and eosin; IL — interleukin; LVEF — left ventricular ejection fraction; LVFS — left ventricular fraction shortening; MIRI — myocardial ischemia-reperfusion injury; OGD/R — oxygen-glucose deprivation/reoxygenation; SD — standard deviation; TNF-α — tumour necrosis factor alpha; TTC — 2,3,5-triphenyltetrazolium chloride.

showed that AEBP1 played its proinflammatory role via enhancement of NF-κB activity through hampering of IκBα [11]. Here, we found a negative relationship between AEBP1 expression and IκBα expression in OGD/R-exposed cardiomyocytes. IκBα protein inhibits NF-κB nuclear translocation via its capacity to bind to

NF-κB subunits, which remains NF-κB in an inactive state in cytoplasm [4]. Upon stimulation, IκBα protein is degraded and separates from NF-κB subunits, thereby leading to nuclear translocation of NF-κB and subsequent transcriptional activation of proinflammatory genes [5]. Similarly, our results suggested that AEBP1 physically interplayed with IκBα via a protein-protein interaction. Interestingly, our findings suggest that AEBP1 loss led to a remarkable increase in IκBα level and reduction in nuclear NF-κB level in cardiomyocytes upon OGD/R stimulation. Remarkably, IκBα knockdown diminished the protection against MIRI caused by AEBP1 deficiency. Collectively, AEBP1--IκBα interaction was crucial for inflammation and apoptosis during MIRI-induced myocardial damage.

Taken together, our observations revealed that AEBP1 promoted the release of pro-inflammatory cytokines and apoptosis induced by MIRI through hampering of IκBα inhibitory function to facilitate NF-κB nuclear translocation. These findings suggest that AEBP1 inhibition possesses cardioprotective effects and may identify as an intervention for MIRI.

ARTICLE INFORMATION AND DECLARATIONS

Data availability statement

The data that support the findings of this study are available from the corresponding author upon reasonable request.

Ethics statement

All animal experiments were carried out in accordance with the NIH guidelines and approved by the Institutional Animal Care and Use Committee of Zhangjiakou First Hospital.

Author contributions

Wei-Na Xue is responsible for the study design, experimental conduct, data analysis, and paper writing.

Funding

None.

Conflict of interest

The author declares that he has no competing interests to disclose.

REFERENCES

1. Bai WW, Wang H, Gao CH, et al. Continuous infusion of angiotensin IV protects against acute myocardial infarction via the inhibition of inflammation and autophagy. Oxid Med Cell Longev. 2021; 2021: 2860488, doi: 10.1155/2021/2860488, indexed in Pubmed: 34950416.
2. Bogachev O, Majdalawieh A, Pan X, et al. Adipocyte enhancer-binding protein 1 (AEBP1) (a novel macrophage proinflammatory mediator) overexpression promotes and ablation attenuates atherosclerosis in ApoE (–/–) and LDLR (–/–) mice. Mol Med. 2011; 17(9-10): 1056–1064, doi: 10.2119/molmed.2011.00141, indexed in Pubmed: 21687917.
3. Fan Z, Cai L, Wang S, et al. Baicalin prevents myocardial ischemia/reperfusion injury through inhibiting ACSL4 mediated ferroptosis. Front Pharmacol. 2021; 12: 628988, doi: 10.3389/fphar.2021.628988, indexed in Pubmed: 33935719.
4. Ghosh S, Baltimore D. Activation in vitro of NF-kappa B by phosphorylation of its inhibitor I kappa B. Nature. 1990; 344(6267): 678–682, doi: 10.1038/344678a0, indexed in Pubmed: 2157987.
5. Ha SE, Bhagwan Bhosale P, Kim HH, et al. Apigetrin Abrogates Lipopolysaccharide-Induced Inflammation in L6 Skeletal Muscle Cells through NF-κB/MAPK Signaling Pathways. Curr Issues Mol Biol. 2022; 44(6): 2635–2645, doi: 10.3390/cimb44060180, indexed in Pubmed: 35735621.
6. Holloway RW, Bogachev O, Bharadwaj AG, et al. Stromal adipocyte enhancer-binding protein (AEBP1) promotes mammary epithelial cell hyperplasia via proinflammatory and hedgehog signaling. J Biol Chem. 2012; 287(46): 39171–39181, doi: 10.1074/jbc.M112.404293, indexed in Pubmed: 22995915.
7. Ju J, Li XM, Zhao XM, et al. Circular RNA FEACR inhibits ferroptosis and alleviates myocardial ischemia/reperfusion injury by interacting with NAMPT. J Biomed Sci. 2023; 30(1): 45, doi: 10.1186/s12929-023-00927-1, indexed in Pubmed: 37370086.
8. Li D, Liu Z, Ding X, et al. AEBP1 is one of the epithelial-mesenchymal transition regulatory genes in colon adenocarcinoma. Biomed Res Int. 2021; 2021: 3108933, doi: 10.1155/2021/3108933, indexed in Pubmed: 34938806.
9. Majdalawieh AF, Massri M, Ro HS. AEBP1 is a novel oncogene: mechanisms of action and signaling pathways. J Oncol. 2020; 2020: 8097872, doi: 10.1155/2020/8097872, indexed in Pubmed: 32565808.
10. Majdalawieh A, Zhang L, Fuki IV, et al. Adipocyte enhancer-binding protein 1 is a potential novel atherogenic factor involved in macrophage cholesterol homeostasis and inflammation. Proc Natl Acad Sci U S A. 2006; 103(7): 2346–2351, doi: 10.1073/pnas.0508139103, indexed in Pubmed: 16461908.
11. Majdalawieh A, Zhang L, Ro HS. Adipocyte enhancer--binding protein-1 promotes macrophage inflammatory responsiveness by up-regulating NF-kappaB via IkappaBalpha negative regulation. Mol Biol Cell. 2007; 18(3): 930–942, doi: 10.1091/mbc.e06-03-0217, indexed in Pubmed: 17202411.
12. Nickelsen A, Götz C, Lenz F, et al. Analyzing the interactome of human CK2β in prostate carcinoma cells reveals HSP70-1 and Rho guanin nucleotide exchange factor 12 as novel interaction partners. FASEB Bioadv. 2023; 5(3):

114–130, doi: 10.1096/fba.2022-00098, indexed in Pubmed: 36876296.
13. Rao M, Wang X, Guo G, et al. Resolving the intertwining of inflammation and fibrosis in human heart failure at single-cell level. Basic Res Cardiol. 2021; 116(1): 55, doi: 10.1007/s00395-021-00897-1, indexed in Pubmed: 34601654.
14. Ren J, Han Y, Ren T, et al. AEBP1 promotes the occurrence and development of abdominal aortic aneurysm by modulating inflammation via the nf-κb pathway. J Atheroscler Thromb. 2020; 27(3): 255–270, doi: 10.5551/jat.49106, indexed in Pubmed: 31462616.
15. Ro HS, Kim SW, Wu D, et al. Gene structure and expression of the mouse adipocyte enhancer-binding protein. Gene. 2001; 280(1-2): 123–133, doi: 10.1016/s0378-1119(01)00771-5, indexed in Pubmed: 11738825.
16. Shao X, Zhang X, Yang L, et al. Integrated analysis of mRNA and microRNA expression profiles reveals differential transcriptome signature in ischaemic and dilated cardiomyopathy induced heart failure. Epigenetics. 2021; 16(8): 917–932, doi: 10.1080/15592294.2020.1827721, indexed in Pubmed: 33016206.
17. Sun W, Wu X, Yu P, et al. LncAABR07025387.1 enhances myocardial ischemia/reperfusion injury miR-205/ /ACSL4-mediated ferroptosis. Front Cell Dev Biol. 2022; 10: 672391, doi: 10.3389/fcell.2022.672391, indexed in Pubmed: 35186915.
18. Thackeray JT, Hupe HC, Wang Y, et al. Myocardial inflammation predicts remodeling and neuroinflammation after myocardial infarction. J Am Coll Cardiol. 2018; 71(3): 263–275, doi: 10.1016/j.jacc.2017.11.024, indexed in Pubmed: 29348018.
19. Toldo S, Mauro AG, Cutter Z, et al. Inflammasome, pyroptosis, and cytokines in myocardial ischemia-reperfusion injury. Am J Physiol Heart Circ Physiol. 2018; 315(6): H1553–H1568, doi: 10.1152/ajpheart.00158.2018, indexed in Pubmed: 30168729.
20. Tsai CF, Lin HW, Liao JM, et al. Alga protects against myocardial ischemia/reperfusion injury by attenuating TLR4 signaling. Int J Mol Sci. 2023; 24(4), doi: 10.3390/ijms24043871, indexed in Pubmed: 36835281.
21. Wang X, Chen J, Huang X. Rosuvastatin attenuates myocardial ischemia-reperfusion injury via upregulating miR-17-3p-mediated autophagy. Cell Reprogram. 2019; 21(6): 323–330, doi: 10.1089/cell.2018.0053, indexed in Pubmed: 31730378.
22. Wu F, Wei H, Hu Y, et al. Upregulation of P2X7 exacerbates myocardial ischemia-reperfusion injury through enhancing inflammation and apoptosis in diabetic mice. J Immunol. 2023; 210(12): 1962–1973, doi: 10.4049/jimmunol.2200838, indexed in Pubmed: 37144844.
23. Wu Z, Bai Y, Qi Y, et al. lncRNA NEAT1 downregulation ameliorates the myocardial infarction of mice by regulating the miR-582-5p/F2RL2 axis. Cardiovasc Ther. 2022; 2022: 4481360, doi: 10.1155/2022/4481360, indexed in Pubmed: 36540097.
24. Xie Bo, Liu X, Yang J, et al. PIAS1 protects against myocardial ischemia-reperfusion injury by stimulating PPAR SUMOylation. BMC Cell Biol. 2018; 19(1): 24, doi: 10.1186/s12860-018-0176-x, indexed in Pubmed: 30419807.
25. Xu Z, Wei Z, Zhu Y, et al. Cardioprotection of mAb2G4/ODN/lip on myocardial ischemia-reperfusion injury via inhibiting the NF-κB signaling pathway. Cardiovasc Ther. 2023; 2023: 5034683, doi: 10.1155/2023/5034683, indexed in Pubmed: 37151220.
26. Zhang GY, Gao Y, Guo XY, et al. MiR-199a-5p promotes ferroptosis-induced cardiomyocyte death responding to oxygen-glucose deprivation/reperfusion injury via inhibiting Akt/eNOS signaling pathway. Kaohsiung J Med Sci. 2022; 38(11): 1093–1102, doi: 10.1002/kjm2.12605, indexed in Pubmed: 36254861.
27. Zhang Q, Lenardo MJ, Baltimore D. 30 years of NF-κB: a blossoming of relevance to human pathobiology. Cell. 2017; 168(1-2): 37–57, doi: 10.1016/j.cell.2016.12.012, indexed in Pubmed: 28086098.
28. Zhang R, Xu L, Zhang D, et al. Cardioprotection of ginkgolide B on myocardial ischemia/reperfusion-induced inflammatory injury via regulation of A20-NF-κB pathway. Front Immunol. 2018; 9: 2844, doi: 10.3389/fimmu.2018.02844, indexed in Pubmed: 30619251.
29. Zhang XJ, Liu X, Hu M, et al. Pharmacological inhibition of arachidonate 12-lipoxygenase ameliorates myocardial ischemia-reperfusion injury in multiple species. Cell Metab. 2021; 33(10): 2059–2075.e10, doi: 10.1016/j.cmet.2021.08.014, indexed in Pubmed: 34536344.